High Glass Transition Temperature Fluoropolymers for Hydrophobic Surface Coatings via RAFT Copolymerization

*Molly Rowe,[1] Guo Hui Teo,[1,2] James Horne,[3] Omar Al-Khayat,[4,5] Chiara Neto[4] and Stuart C. Thickett[1,2]**

[1]Centre for Advanced Macromolecular Design (CAMD), School of Chemical Engineering, University of New South Wales, Sydney, NSW 2052 Australia

[2]School of Physical Sciences (Chemistry), University of Tasmania, Sandy Bay TAS 7005 Australia

[3]Central Science Laboratory, University of Tasmania, Sandy Bay TAS 7005 Australia

[4]School of Chemistry F11, The University of Sydney, Sydney, NSW 2006 Australia

[5]School of Chemical and Biomolecular Engineering J01, The University of Sydney, NSW 2006 Australia

Corresponding Author

* Stuart Thickett: stuart.thickett@utas.edu.au Phone: +61-3-6226-2783; Fax: +61-3-6226-2758

ABSTRACT

The preparation of polymer thin films or surface coatings that display a static water contact angle > 95 ° often require hierarchical roughness features or surface functionalization steps. In addition, inherently hydrophobic polymers such as fluoropolymers often possess relatively low glass transition temperatures, reducing their application where thermal stability is required. Herein, the first reported synthesis of 2,3,4,5,6-pentafluorostyrene (PFS) and *N*-phenylmaleimide (NMI) via reversible addition-fragmentation (RAFT) mediated free radical polymerization is presented, with a view towards the preparation of inherently hydrophobic polymers with a high glass transition temperature. A suite of copolymers were prepared and characterized, and due to the inherent rigidity of the maleimide group in the polymer backbone and π-π interactions between adjacent PFS and NMI groups, very high glass transition temperatures were achieved (up to 180 °C). The copolymerization of *N*-pentafluorophenylmaleimide was also performed, also resulting in extremely high glass transition temperature copolymers, however these polymers did not exhibit characteristics of being under RAFT control. Thin films of PFS-NMI copolymers exhibited a static contact angle ~ 100 °, essentially independent of the amount of NMI incorporated into the polymer.

INTRODUCTION

The wettability of a solid surface, such as a polymeric thin film, is a property that is governed by both the chemical composition of the surface and the presence of topographical features.[1] Research into hydrophobic polymer surface coatings has become popular in recent times due to the potential for these coatings to provide an enhancement of performance across a wide range of fields. Hydrophobic surfaces are typically defined as those that have a water static contact angle (θ_{eq}) greater than 90°. This characteristic, in addition to low contact angle hysteresis (the difference between advancing and receding contact angle), make hydrophobic coatings attractive for self-cleaning[2] and anti-fouling[3] applications, and for the prevention of the degradation of materials due to harsh environmental conditions.[4] Hydrophobic surface coatings are also desirable for applications where wettability contrast is required, such as in the preparation of nano- or micropatterned surfaces.[5]

Typically the preparation of hydrophobic polymer surfaces has involved the use of a polymer with a low surface energy (i.e. an inherently hydrophobic polymer),[6] the introduction of hierarchical surface structures,[7] surface functionalization[8] or a combination of all of these.[9] The introduction of surface structures and surface functionalization limits the ease with which these surfaces can be used on a large scale. Additionally, a number of these techniques are also unsuitable for use on non-planar substrates. A popular route to the preparation of hydrophobic polymers is fluorination.[10] However, fluorinated polymers tend to have low glass transition temperatures (e.g. poly(2,3,4,5,6-pentafluorostyrene) ~ 80 °C,[11] poly(vinylidene fluoride) ~ −35 °C,[12] poly(2,2,2-trifluoroethyl methacrylate) ~ 74 °C,[13] poly(hexafluoroisopropyl methacrylate) ~ 69 °C[13b]), which limits their utility for high temperature applications.

The T_g of a given polymer is highly dependent on the ease of chain rotation and the nature of the configuration of functional groups either attached to or incorporated within the polymer chain backbone.[14] Highly rigid polymer chains that are neither readily mobile nor able to move via reptation have high T_g values compared to those that easily undergo bond rotation. Hence, by increasing the chain stiffness of a polymer, the T_g can be increased. It is generally accepted that polymer chain backbones based on single C-C and C-O bonds are relatively flexible compared to backbones with incorporated ring structures.[15] These ring structures are known as 'stiffening groups,' which increase the energy required for bond rotation, subsequently leading to an increase in T_g. As a result, specifically designed copolymers that are both intrinsically hydrophobic (i.e. contain fluorinated groups) and possess vinylic ring structures along the backbone represent a route towards the preparation of hydrophobic surface coatings with a high glass transition temperature.

One particular class of ring-containing monomers that has attracted interest in recent times are *N*-substituted maleimides,[16] a class of electron-poor monomers that result in homopolymers and copolymers with exceptional thermal stability and chemical resistance. Maleimide homo- and copolymers possess particularly high glass transition temperatures[16d] due to the restriction in chain mobility upon incorporation of the 5-membered ring into the polymer backbone. The commercially available *N*-phenylmaleimide (NMI) is known to undergo alternating copolymerization with styrene and produces a resultant copolymer with excellent thermal stability;[17] other substituted maleimides have also been studied for incorporation into polymeric structures via various synthetic strategies.[16b-e] *N*-pentafluorophenylmaleimide (PFPMI), a monomer that contains both hydrophobic and chain-stiffening groups in the same structure, was first reported by Barrales-Rienda *et al.*[18] and has been homo- and copolymerized (with methyl

methacrylate) by Lou *et al.*[16f] to yield high glass-transition temperature polymers with specific optical properties; the hydrophobicity of these materials however was not evaluated. The homopolymerization of *N*-substituted maleimides is generally poor,[16g] and so suitable comonomers for specific applications are needed.

One vinyl homopolymer that is inherently hydrophobic is the polymer of 2,3,4,5,6-pentafluorostyrene (PFS), the surface of which has been shown to possess a high static contact angle ($\theta_{eq} \sim 100°$) and minimal contact angle hysteresis.[19] PFS is an electron poor monomer due to the electronegativity of fluorine, and is known to polymerize with electron-rich monomers (such as styrene) in an alternating manner.[20] This behaviour has been shown by Pugh *et al.*[21] to be due to π-π interactions between arenes and fluoroarenes (such as styrene and PFS) that possess molecular quadrupoles that are approximately equal in magnitude but opposite in sign, promoting association during the copolymerization process. It is anticipated that π-π interactions would exist in the copolymerization of PFS and an appropriately substituted maleimide such as NMI, however this specific concept has not been examined. PFS and NMI have been previously copolymerized using both free-radical and microwave initiation,[6] with reported reactivity ratios indicating a preference for cross-propagation.

In numerous applications, the ability to systematically control the molecular weight of a copolymer is highly desirable. Such control has been developed in recent times through the advent of reversible deactivation radical polymerization (RDRP) techniques such as reversible addition-fragmentation chain transfer (RAFT) polymerization,[22] atom transfer radical polymerization (ATRP)[23] and nitroxide-mediated polymerization (NMP).[24] In all of these techniques, a particular polymer chain length is able to be targeted through the molar ratio of monomer(s) to specific control agent; RAFT is typically considered the most versatile of the

RDRP techniques due to its ability to mediate the polymerization process for a wide range of monomers of differing reactivity. Alternating copolymers of styrene and NMI have been prepared via ATRP,[25] poly(NMI) and poly(styrene-*block*-NMI) have been prepared by dithiobenzoate-medaited RAFT polymerization,[26] and recently Yang *et al.* reported the RAFT synthesis of a styrene-NMI copolymer in the context of polymerization-induced self assembly.[27] To our knowledge, PFS and NMI have not been copolymerized previously via the RAFT process. In addition, PFPMI has never been copolymerized using RAFT-mediated polymerization, nor has the copolymerization of PFPMI with PFS ever been previously reported. In this work, we report the synthesis, characterization and properties of NMI-PFS copolymers prepared via RAFT-mediated solution polymerization across a range of comonomer ratios, in addition to PFPMI-based copolymers prepared using a similar approach. The performance of these polymers with respect to wettability and thermal properties was examined, in particular as a function of copolymer composition.

RESULTS AND DISCUSSION

Synthesis and Characterization of Copolymers via RAFT Polymerization

In this work, copolymers of PFS and a substituted maleimide (either NMI or PFPMI) were prepared via RAFT-mediated solution polymerization and subsequently characterized (see Scheme 1). In the case of PFS/NMI copolymerization, a suite of copolymers were prepared ranging from 0 – 0.5 mole fraction of NMI in the monomer feed, in order to ultimately examine the influence of copolymer composition on both thermal properties of the polymer and its hydrophobicity as a surface coating (see Table 1).

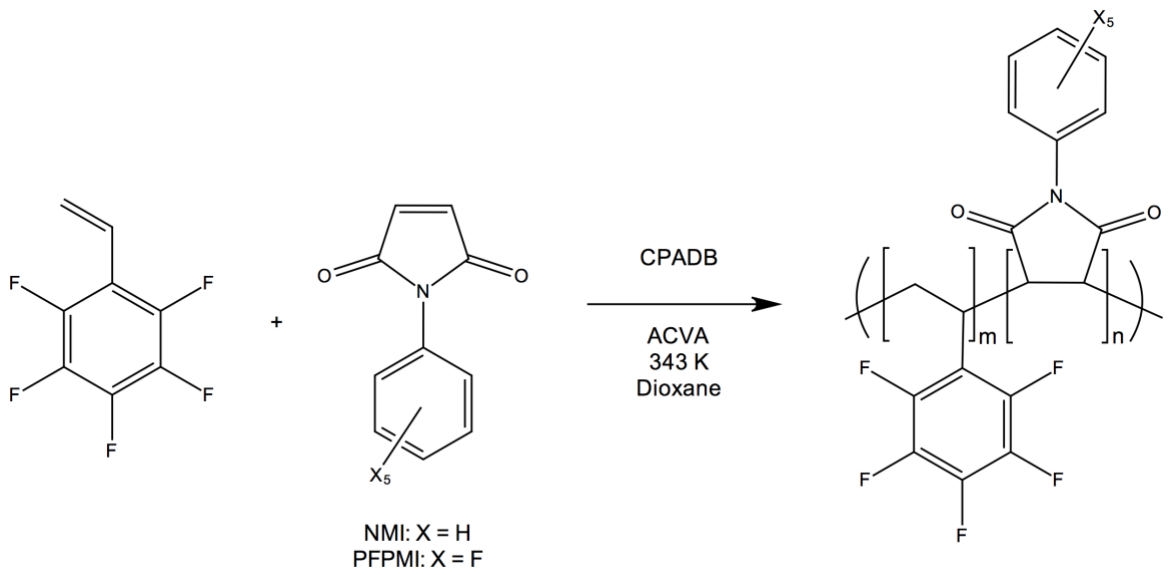

124

125 **Scheme 1.** Reaction scheme for the RAFT-mediated copolymerization of PFS and NMI/PFPMI. Styrene was used in
126 place of PFS in Sample 8.

127

Table 1. Details of RAFT mediated polymerization of PFS-NMI copolymers, conversion and molecular weight data and thermal properties.

NMI-Based Copolymers									
Sample	**Mole Fraction NMI (Feed)**	**Conversion [a] (NMI/PFS)**	**Mole Fraction NMI in Copolymer (conversion)**	**Mole Fraction NMI in Copolymer (XPS)**	**Predicted Mole Fraction NMI in Copolymer[b]**	M_n [c] **(kDa)**	$Đ$	T_g **(°C)**	T_{10} / T_{50} [d] **(°C)**
1	0	0/0.25	0	0	0	16.4	1.23	93	405/468
2	0.10	0.28/0.26	0.11	0.12	0.10	12.3	1.24	109	379/447
3	0.20	0.33/0.36	0.19	0.18	0.20	10.6	1.18	130	361/409
4	0.30	0.34/0.31	0.32	0.22	0.27	9.8	1.19	133	364/423
5	0.40	0.46/0.58	0.35	0.34	0.34	12.7	1.26	149	348/398
6	0.50	0.56/0.62	0.47	0.37	0.41	25.0	1.24	180	389/427

PFPMI-Based Copolymers								
Sample	**Mole Fraction PFPMI (Feed)**	**Conversion[a] (PFPMI/ other)**	**Mole Fraction PFPMI in Copolymer (conversion)**	**Mole Fraction PFPMI in Copolymer (XPS)**	M_n [c] **(kDa)**	$Đ$	T_g **(°C)**	T_{10} / T_{50} [d] **(°C)**
7 (PFPMI-PFS)	0.29	0.29/0.55	0.18	0.25	23.5	2.68	145	373/414
8 (PFPMI-PS)	0.30	0.83/0.49	0.42	0.46	39.7	2.07	193	371/405

[a] Determined from ^{1}H NMR spectra taken after polymerization, [b]Predicted based on reactivity ratios elucidated by Agarwal *et al*[6], [c]Measured relative to poly(styrene) standards via calibration, [d]The temperature required to reach 10% and 50% mass loss respectively.

Copolymers of PFS and NMI were found to have number-average molecular weight ranging from 9.8 to 25 kDa (relative to linear polystyrene standards) and, with the exception of the PFS homopolymer (Sample 1), possessed monomodal molecular weight distributions (see Table 1 and Figure 1A). SEC analysis of all PFS-NMI copolymers revealed relatively narrow dispersities ($Đ \leq$ 1.26 in all cases). There was no obvious correlation between M_n and comonomer composition, which differs from the work of Agarwal *et al.*,[6] where molecular weight was shown to increase with increasing mole fraction of NMI in an AIBN-initiated solution polymerization. There was an increase in the fractional conversion of both monomers upon increasing the mole fraction of NMI (see Table 1), suggesting a co-operative effect in the copolymerization of the two monomers.

The copolymerization of PFPMI with PFS and styrene (Samples 7 and 8 in Table 1) yielded polymers with M_n = 23.5 kDa and M_n = 39.7 kDa respectively with effective incorporation of both monomers, however the molecular weights distributions were comparatively broad ($Đ$ = 2.68 and 2.07 respectively; see Figure 1B). These dispersities are significantly higher than would be expected for a RAFT-mediated polymerization,[22a] and the attempted chain extension of Sample 8 with additional styrene was unsuccessful (i.e. there was no evolution of the molecular weight distribution). These results indicated potential loss of the dithiobenzoate end-group during polymerization, preventing effective control over the resultant molecular weight distribution. We postulate that residual impurity from the PFPMI synthesis (*N*-pentafluorophenylmaleamic acid) may have degraded the CPADB in solution, resulting in an uncontrolled radical polymerization, as observed here.

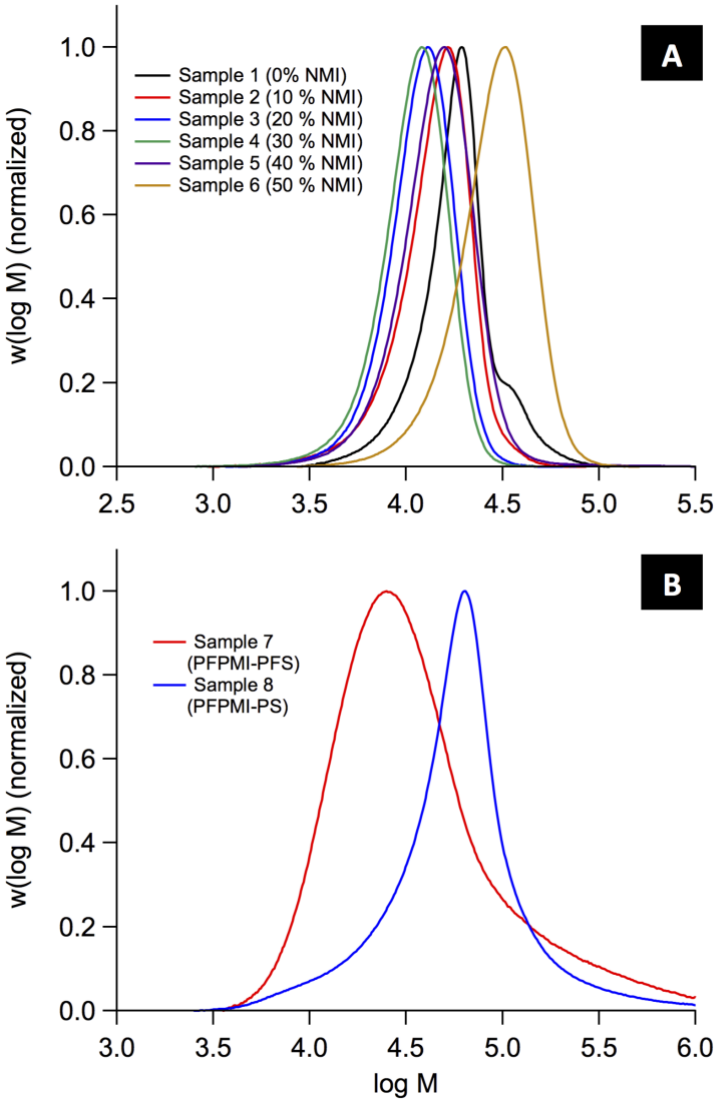

149

150 **Figure 1.** Height normalized SEC distributions of A) Six PFS and NMI polymer samples described in Table 1, B)
151 PFPMI copolymer samples described Table 2.

152

153 Characterization of the copolymers was further performed using ^{1}H and ^{19}F NMR spectroscopy,
154 in addition to XPS, in order to confirm the chemical composition of the polymers. Determination
155 of fractional conversion of the two monomers typically indicated a slight enrichment of PFS
156 units in the copolymer, which was more apparent at higher mole fractions of NMI. This was in
157 good agreement with the composition as determined by XPS, where the F/N atomic ratio was

used to calculate the copolymer composition (see Figure S1 and Table S1 in Supporting Information). The slight enrichment in PFS is expected based on the published reactivity ratios for NMI/PFS copolymerization of r_1 (NMI) = 0.28 and r_2 (PFS) = 0.86, which confirms the preference for PFS to add to a growing polymer chain.[6] The instantaneous copolymer compositions (as predicted by the Lewis-Mayo equation using these reactivity ratios) were in good agreement to the experimentally determined composition (see Table 1). The reactivity ratios are postulated to be due to significant steric hindrance around the NMI unit during chain propagation, in addition to the resonance stabilization generated from a terminal PFS radical. As the product of the two reactivity ratios is 0.24 and both values are low, PFS and NMI have a tendency towards alternation and are more likely to cross-propagate with each other, rather than self-propagate.[28] Analysis of the PFPMI-based copolymers (Samples 7 and 8) showed highly different behaviour depending on whether PFS of styrene was the co-monomer; copolymerization with PFS resulted in an enrichment of PFS in the polymer, whereas PFPMI was enriched in the polymer relative to the feed when styrene was used. The aliphatic region of the ^{1}H NMR spectrum of all copolymers consisted of the anticipated resonances of backbone protons due to PFS (between 1.5 and 2.8 ppm) and NMI/PFPMI (between 3.0 and 4.2 ppm) units in the polymer chain.[6, 21, 26]

The tendency for alternating copolymerization of PFS and NMI can potentially be explained in terms of π-π interactions between the aromatic ring of NMI and the fluorinated aromatic ring of PFS. The highly electronegative nature of fluorine means that significant electron density is shifted away from the ring, resulting in a quadrupole moment (see Scheme 2). The aromatic ring in the NMI results in the formation of a quadrupole moment that is similar in magnitude, but opposite in sign to that of the perfluoroarene[29]. The result of the polarization of these ring

systems is an intermolecular interaction that is of "similar strength to a weak hydrogen bond"[21, 29a]. Pugh *et al* have reported that the strength and extent of π- π interactions between arenes and perfluoroarenes correlated with the tendency of their vinyl analogues (e.g. styrene, PFS) to alternate during copolymerization. [21] As a consequence, despite these monomers both being electron deficient, it is likely that NMI and PFS copolymerize in an alternating as a result of π- π interactions; such interactions are also anticipated for the PFPMI-PS copolymer (Sample 8).

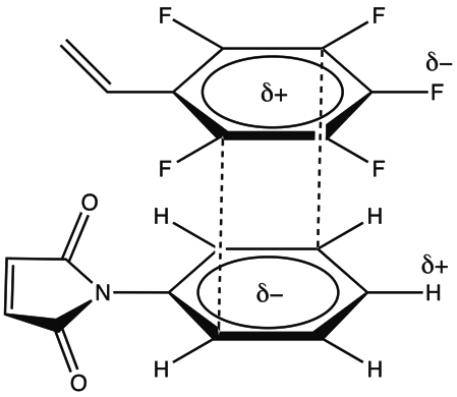

Scheme 2. Schematic showing the hypothesized π-π interaction between PFS and NMI

Spectroscopic evidence (NMR and FTIR spectroscopy) supports the hypothesis that copolymers with increasingly alternating character are formed on the basis of π-π interactions. The ^{19}F NMR spectra of the copolymers showed a broadened chemical shift range and the appearance of additional resonances downfield (shifted approximately 1 - 2 ppm) relative to the PFS homopolymer, upon increasing the amount of NMI units incorporated into the polymer (see Figure 2A). It is likely that these additional peaks are due to the increased probability of adjacent PFS-NMI units in the polymer backbone, due to π-π interactions between adjacent PFS and NMI units; Pugh *et al.* reported similar resonance shifts in the ^{19}F spectra of PFS-styrene copolymers[29b]. FTIR analysis indicated that, relative to the spectrum of the homopolymer of

NMI, the carbonyl stretch of the maleimide group at approximately 1700 cm^{-1} was blueshifted ~ 15-20 cm^{-1} when PFS was present in the copolymer (see Figure 2B). The blue-shifting of this peak is characteristic of systems where stacking interactions occur.[30]

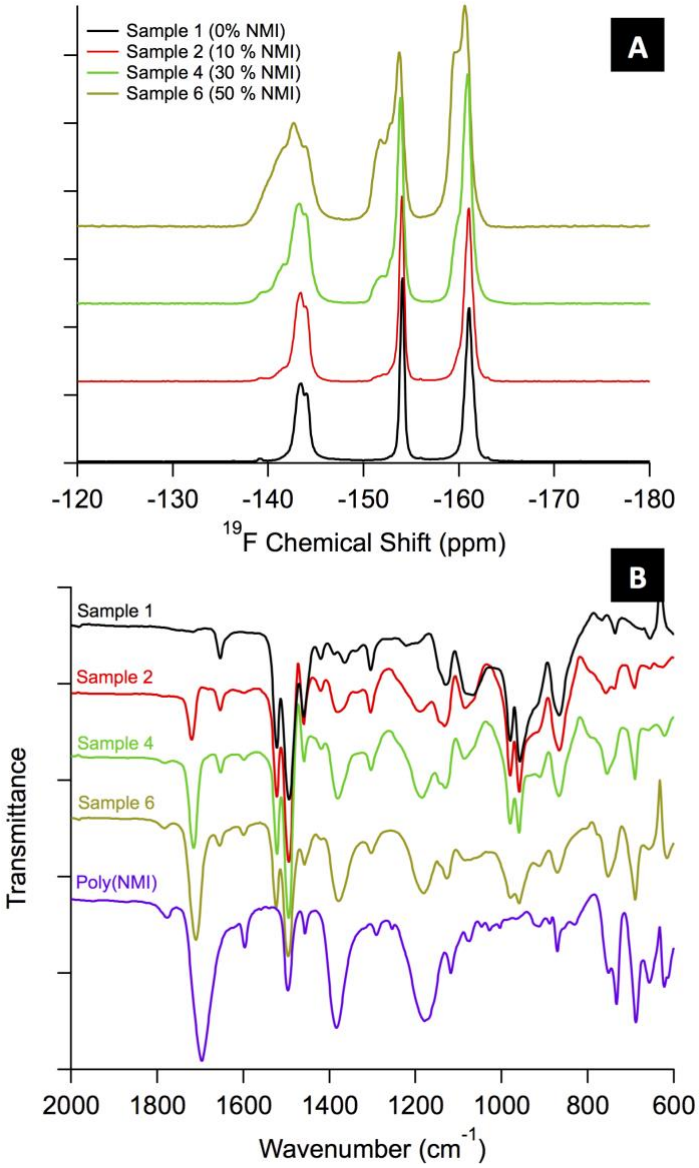

Figure 2. A) ^{19}F NMR and B) FTIR spectra for PFS-NMI copolymers described in Table **1**. The purple FTIR spectrum corresponds to the homopolymer of NMI (M_n = 6 kDa).

A series of further NMR observations were made to establish the connectivity between protons in both the PFS and NMI subunits for Sample 6, which consists of roughly equal proportions of the monomers (PFS:NMI mole ratio = 63:37). The relatively large size of the polymer leads to broadened spectral lineshape due to efficient relaxation and likely slow overall correlation time. Nevertheless, we were able to record 2D ^{1}H-^{1}H NOESY data, ^{1}H-^{13}C HSQCme/HMBC spectra and ^{19}F-^{13}C HSQC/HMBC spectra to assist our interpretation of the data (see Figures S3 – S7, Supporting Information). The ^{1}H-^{13}C HSQCme experiment (Figure S3) unambiguously identified the methylene resonances of the linker via the multiplicity editing step. ^{1}H-^{1}H NOESY correlations (Figure S4) within the aliphatic region are consistent with a network of connectivities existing between methine groups in NMI and the methine group in PFS, with the methylene protons between. Crosspeaks are broad however, and are assumed to represent a range of possible pairings of monomer units and their resultant ^{1}H chemical shifts. This is consistent with the range of chemical shifts observed in the ^{19}F 1D spectrum shown in Figure 2A. This does not preclude possible conformational states also being present, but it is reasonable to assume based on the work of Pugh *et al.*[21] that multiple pairing arrangements are the main source of extra signals in this case. The aromatic systems of PFS and NMI are well characterized in 2D ^{1}H/^{19}F-^{13}C correlation experiments (Figures S5 and S6). Splitting of carbon signals in the ^{13}C 1D spectrum is observed for PFS due to the ^{13}C-^{19}F fluorine couplings ($^{1}J_{CF}$ 250Hz, $^{2}J_{CF(para)}$ 90 Hz, see Figure S2). Correlations between carbonyl carbons and both NMI methine protons and PFS methylene protons were observed in ^{1}H-^{13}C-HMBC spectra (Figure S7). A range of long-range coupling constant values were trialed in the ^{1}H-^{13}C HMBC experiment, with a 10 Hz value being the most information rich.

Thermal Properties

The glass transition temperature (T_g) of the PFS-NMI copolymers was found to increase significantly with the incorporation of NMI as comonomer. The T_g increased from 93°C for pure PPFS to 180°C for the copolymer with 37 mol% NMI (Sample 6; see Table 1). The increase in the T_g of copolymers with increasing NMI content was anticipated due to the fact that chain stiffening groups within the polymer backbone, such as the five-membered maleimide ring in NMI, increase the glass transition temperature of the resultant polymer.[15] It is worth noting however that the measured T_g values were significantly greater than the values predicted by the Fox equation (see Figure 3A), up to 57 °C greater for Sample 6 which contained the greatest content of NMI. The Fox equation is an empirical expression that is best suited for situations in which the glass transition temperatures of both polymers are similar,[31] and given the large difference in reported T_g values for PFS and NMI homopolymers (80 °C and 325 °C respectively), the application of the Fox equation in this instance may not be valid.[11, 19, 32] However in this particular system, such an elevation in T_g is further indication of stacking interactions between NMI and PFS units in the polymer backbone. Pugh *et al.* reported elevated T_g's for copolymers of styrene and PFS relative to predicted values, which they attributed to intramolecular π-π interactions[21]. Such interactions would increase the stiffness of the PFS-NMI copolymer chains, which would lead to a further increase in T_g in addition to the increase caused by the incorporation of NMI. This explanation is further supported by the fact that the deviation of the T_g from predicted is greatest when the PFS:NMI ratio approaches unity.

T_g values for the PFS-PFPMI and styrene-PFPMI copolymers were found to be 145 °C and 193 °C respectively (see Table 1). Given that the T_g of poly(styrene) is 107 °C, [33] it is clear that the incorporation of PFPMI into the backbone of both copolymers backbone increases the T_g quite

significantly (there are no reported literature values for the homopolymer T_g of PFPMI). One would anticipate that, in the case of PS-PFPMI, intramolecular π-π interactions would exist in this system given the arene and fluoroarene groups present in the copolymer.[29a] This would have the effect of stiffening the polymer chains and increasing the T_g to a value greater than would be predicted purely on the composition of the polymer.

Thermogravimetric analysis revealed that the PFS-NMI copolymers undergo a fairly rapid decomposition at high temperature and that the incorporation of NMI results in a second, more gradual decomposition at high temperatures (see Figure 3B). Relative to the PFS homopolymer, the incorporation of NMI leads to a significant reduction of ~ 40 °C in the temperature where the first, rapid decomposition occurs (see Table 1). NMI-based polymers are reported to have two possible mechanistic pathways to degradation; (i) random chain scission preceding inter- and intra-molecular hydrogen radical transfer, and (ii) imide-isoimide rearrangement followed by the ejection of CO_2[34]. The formation of imides upon thermal degradation of copolymers containing NMI units is a potential cause of the more gradual copolymer decomposition at high temperatures with an increasing proportion of NMI units.[6] TGA of the PFPMI copolymers showed a two-stage decomposition profile, and it is anticipated that these copolymers undergo a similar thermal degradation process given the structural similarity of PFPMI and NMI (see Figure S8, Supporting Information).

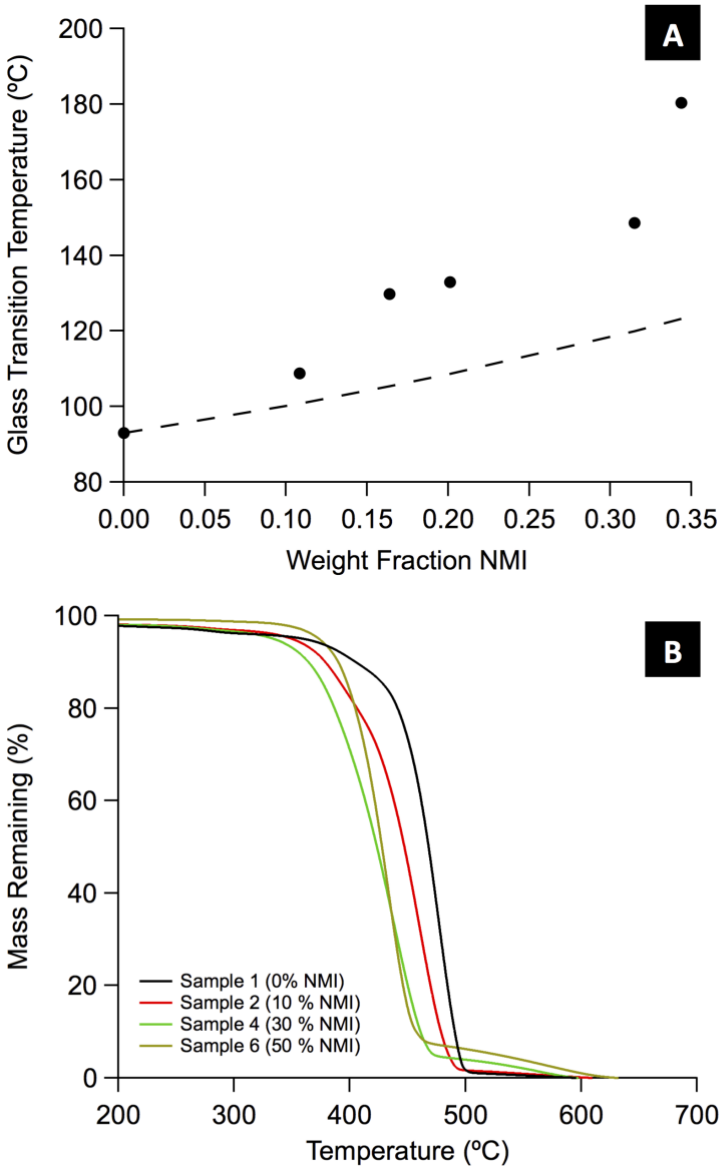

Figure 3. A) Relationship between the bulk Tg and the proportion of NMI in the PFS-NMI copolymer(dotted line represents the Fox equation prediction), B) TGA decomposition profiles of PFS-NMI copolymers outlined in Table 1.

Thin Film Fabrication and Wettability.

Thin films were prepared via spin coating of the PFS homopolymer and PFS-NMI copolymer from acetone at a concentration of 10 mg mL^{-1}. For the majority of these layers, the film thickness was not able to be determined via ellipsometry due to the extremely poor fit of the obtained data to a monolayer model with Cauchy absorption profile. A good ellipsometric fit was obtained for Sample 6 (Figure S9, Supporting Information), with an estimated film thickness of ~ 41.8 (± 0.3) nm. The poor fit for the majority of surfaces was attributed to the roughness of the as-prepared surfaces relative to the apparent thickness of the films, [35] as confirmed by AFM topographical analysis.

The R_{RMS} values of the as-prepared films generally decreased with an increasing proportion of NMI in the copolymer surfaces, from 48.5 nm for pure PPFS to 10.7 nm for the copolymer surface with 37 mol % NMI (see Figure 4); these are very high compared to the RMS roughness values of polymer films such as polystyrene on Si wafers prepared by spin coating (R_{RMS} < 0.5 nm). AFM analysis of all PFS-NMI copolymer thin films revealed highly structured surfaces, with troughs being almost 30 nm deep for the surface with the highest proportion of NMI (see Figure S10, Supporting Information). The regularity of the structuring appears to increase with an increasing proportion of NMI in the copolymer thin film (Figure S11, Supporting Information), and the reason for this structuring is at this stage unclear. Acetone was used as the spin-coating solvent, and it is known that films prepared from polymer solution with high vapour pressure are typically rougher than solvents that evaporate less quickly;[36] Strawhecker *et al* attribute this characteristic to the creation of Marangoni instabilities coupled with the inability of the resulting polymer film to level adequately before it becomes "frozen" into a dried state[36b]. The increasing amount of π-π interactions between PFS and NMI units when these polymers are

297 prepared as a film (both inter- and intramolecular interactions) may also partially explain the
298 observed surface structuring.

299 Static and dynamic water contact angle measurements were performed on the as-cast films. It
300 was anticipated that the contact angle would decrease upon incorporation of NMI due to polar
301 groups in the maleimide unit, however no obvious trend in the static contact angle was observed
302 (see Table 2). In addition, the measured static contact angles reported here were lower than those
303 reported by Agarwal *et al.,*[6] who prepared films from a 50:50 v/v mixture of THF and
304 dimethylformamide. We attribute the variation in these contact angle values to the high degree of
305 roughness and structuring present within the polymer film. To address this issue, the PFS-NMI
306 films were thermally annealed for an hour at a temperature 20 °C greater than the bulk T_g of the
307 copolymer, in order to allow polymer chains within the film to move towards their equilibrium
308 conformation. This annealing step resulted in a significant increase in the static contact angle of
309 all surfaces studied (see Table 2 and Figure 4), as well as an increase in the advancing and
310 receding contact angles (with a reduction in contact angle hysteresis). The variation in the static
311 contact angle as a function of NMI content was extremely small, with a measured contact angle
312 of 101.7 ° for the PFS homopolymer, through to 96.8 ° for Sample 6 (with the highest NMI
313 content). It is hypothesized that regardless of copolymer composition, the lower surface energy
314 fluorinated groups from the PFS were able to migrate to the polymer-air interface upon thermal
315 annealing,[37] and upon cooling this new surface morphology was maintained. Surface structuring
316 was removed or greatly reduced post-annealing (see Figure 4), which supports the concept of
317 chain reorganization when heated above the T_g. This result demonstrates the facile method that
318 thermal annealing represents in the preparation of hydrophobic, highly glassy copolymers.

Both as-cast PFPMI copolymer thin films had static contact angles with water that were greater than 90° and relatively low contact angle hystereses compared to that of the PFS-NMI surfaces (see Table 2). The highly fluorinated PFS-PFPMI copolymer surface had the higher static contact and lower contact angle hysteresis compared to the styrene-PFPMI surface, however there was little benefit with respect to increased contact angle relative to NMI-based copolymer films. These films were also shown to delaminate upon exposure to water for more than five minutes, a phenomenon which was suppressed upon thermal annealing of the films in a manner analogous to the PFS-NMI copolymers. There was only a minor change in the static contact angle upon thermal annealing of PFPMI-based surfaces, coupled with no significant variation in surface topography or roughness (see Figure S12, Supporting Information).

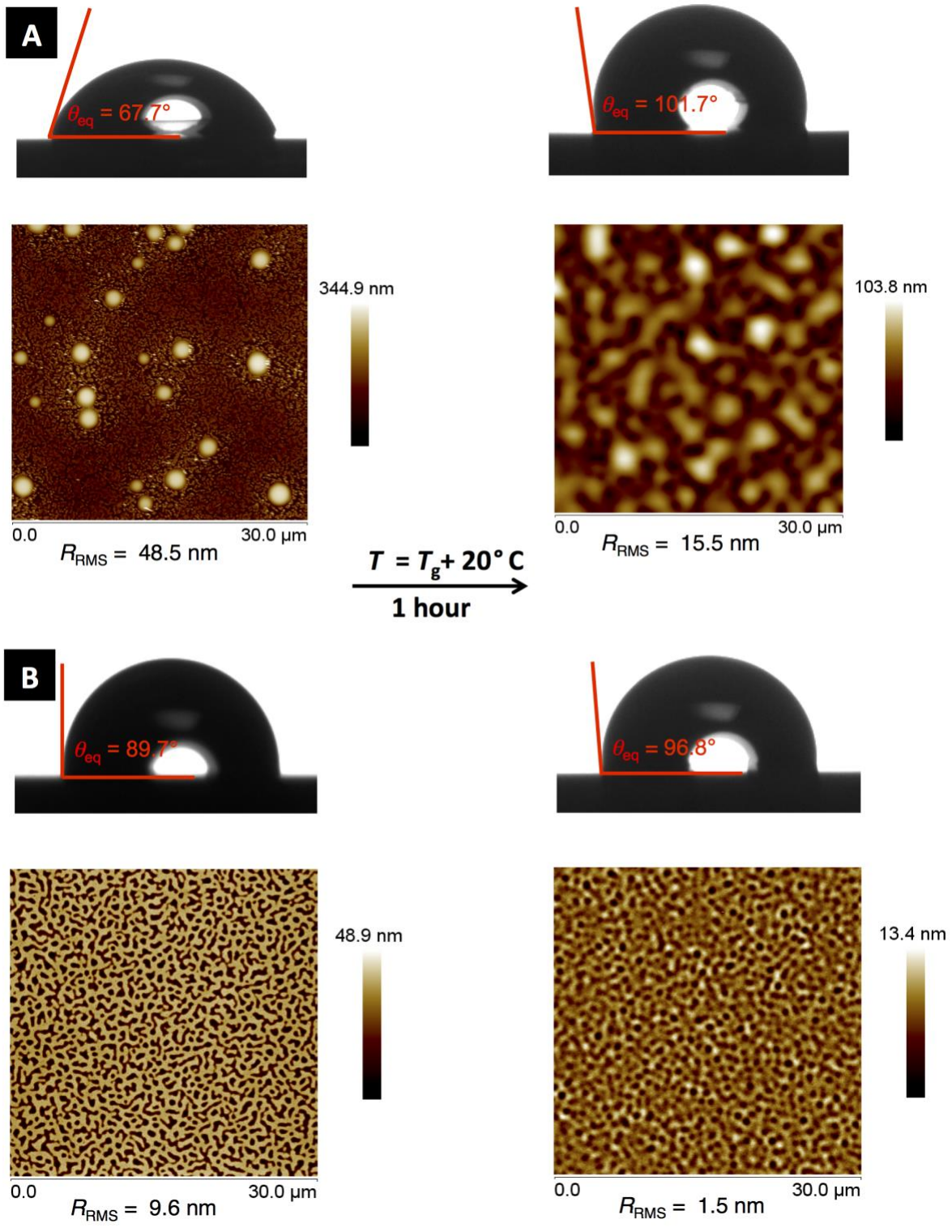

329

330 **Figure 4.** Static contact angle of water on surfaces (θ_{eq}), AFM image of polymer surfaces and roughness (R_{RMS}) pre-
331 (left) and post-annealing (right); A) PPFS homopolymer thin film, B) PFS-NMI copolymer surface with 37 mol%
332 NMI (Sample 6).

Table 2. Static and dynamic water contact angle data for PFS-NMI and PFPMI-based copolymers.

	As-Cast		Post-Annealing	
Sample	**Static Water CA (°)**	**Hysteresis (°) (Advancing/ Receding)**	**Static Water CA (°)**	**Hysteresis (°) (Advancing/ Receding)**
1	67.7 ± 0.3	43.1 (85.2/42.1)	101.7 ± 0.2	29.2 (109.8/80.6)
2	93.3 ± 0.5	38.2 (102.8/64.6)	98.2 ± 1.7	14.2 (102.1/87.9)
3	77.4 ± 1.2	53.4 (80.3/26.9)	101.3 ± 0.5	34.5 (99.8/65.3)
4	86.8 ± 1.0	37.5 (89.8/52.4)	102.7 ± 1.3	23.9 (98.9/75.0)
5	69.1 ± 0.4	[a]	85.0 ± 5.0	27.5 (86.8/59.3)
6	89.7 ±1.8	[a]	96.8 ± 0.4	27.9 (98.3/70.4)
7	96.0 ± 0.4	29.7 (98.9/69.1)	99.5 ± 0.9	25.5 (100.8/75.3)
8	91.1 ± 1.8	33.5 (95.2/61.8)	86.3 ± 0.9	21.9 (87.4/65.5)

[a]Not measured

CONCLUSIONS

In this work, hydrophobic copolymers with high glass transition temperatures have been successfully prepared using via RAFT-mediated free-radical polymerization. The successful RAFT copolymerization of 2,3,4,5,6-pentafluorostyrene (PFS) and *N*-phenylmaleimide (NMI) is reported for the first time, with copolymers of narrow molecular weight distributions ($Đ \leq 1.26$ in all cases) and compositions that were in good agreement with monomer feed composition and established reactivity ratios. Spectroscopic characterization of these copolymers (NMR and FTIR spectroscopy) demonstrated evidence of π-π stacking interactions between adjacent PFS and NMI units within the polymer backbone; these interactions had the additional, beneficial effect of greatly increasing the measured glass transition temperature relative to predicted values. The highest T_g value reported was 180 °C for a copolymer with 37 mol % NMI, a value due to the chain stiffness from incorporation of the rigid maleimide group as well as stacking interactions.

In an attempt to synthesize polymers with an even greater fluorine content and potential hydrophobicity, *N*-pentafluorophenylmaleimide (PFPMI) was synthesized and copolymerized with PFS and styrene. The resultant polymers possessed very high glass transition temperatures as expected, however attempts to produce polymers with narrow molecular weight distributions via RAFT polymerization were unsuccessful. Both copolymers had dispersity values > 2, and chain extension was not successful. This result was attributed to partial degradation of the RAFT agent, as opposed to inappropriate choice of chain transfer agent, given the previous success of preparing low dispersity PFS-NMI copolymers.

When prepared as spin-cast films, PFS-NMI copolymers demonstrated highly structured and rough surfaces by atomic force microscopy. These surface features were reduced upon thermal

annealing of the films, which additionally resulted in an increase in the water static contact angle of the surfaces. Despite up to 37 mol % NMI present in the polymer backbone, the surfaces were hydrophobic and displayed a static contact angle only a few degrees lower than that of the PFS homopolymer. This result demonstrates a potentially simple method of preparing hydrophobic polymer surface coatings that also possess a very high glass transition temperature, which is uncommon. We anticipate that, given their high glass transition temperature, thermal stability and hydrophobic nature, these materials will be of interest for surface coatings where both hydrophobicity and long-term stability are required, such as environmentally protective coatings, self-cleaning materials and anti-fouling surfaces.

EXPERIMENTAL SECTION

Materials. All chemicals were used as received unless otherwise stated. 2,3,4,5,6-pentafluorostyrene (PFS, >98% purity, stored at 4°C before use) and 2,3,4,5,6-pentafluoroaniline (> 98%) were purchased from Alfa Aesar. Synthesis grade maleic anhydride (> 99%) was purchased from Scharlau. 4-cyano-4-(phenyl-carbonothioylthio) pentanoic acid (CPADB) RAFT agent (> 97%), 4-4'-azobis(4-cyanovaleric acid) (ACVA) initiatior (> 96%), *N*-phenylmaleimide (NMI, >97% purity), anhydrous 1,4-dioxane solvent (> 99.8% purity) and styrene (> 99% purity) were all purchased from Sigma-Aldrich, styrene was purified further by passing over a column of basic alumina and stored at 4°C before use. Distilled ethanol, acetone (both Chem Supply) and tetrahydrofuran (> 99.9% purity, Merck Millipore) were used as solvents for spin coating. All 1 cm_2 silicon wafers were diamond cut from a larger, prime grade polished silicon wafer supplied by MMRC Pty Ltd, Australia.

Synthesis of *N*-pentafluorophenyl maleimide. The synthesis of *N*-pentafluorophenyl maleimide (PFPMI) followed the general procedure of Lou *et al.*[16f] In a 50 mL three-necked flask containing a stirrer and fitted with a dropping funnel and reflux condenser, 2.684 g (0.0274 mol) of maleic anhydride and 14 mL of 1,4-dioxane were combined. 9 mL of 1,4-dioxane was added to 5.0 g (0.0273 mol) of 2,3,4,5,6-pentafluoroaniline and this solution was then added dropwise to the flask over 10 minutes. The reaction mixture was refluxed for 96 hours at 105°C. Approximately half of the 1,4-dioxane was removed then removed, an equivalent volume of toluene was added and the mixture continuously refluxed at 110°C for 3 hours. Two-thirds of the solvent was then removed. 25 mL of acetic acid was added to the flask and the reaction mixture was refluxed at 125°C under argon for 18 hours. The resultant solution was precipitated added to ice-cold water and the precipitated solid collected by vacuum filtration. The precipitated solid was recrystallised twice from a 1:4 ethanol/hexane solution, collected by vacuum filtration and dried in a vacuum oven for 18 hours at 30°C. The yield was 47 %. ^{1}H NMR ($CDCl_3$, 400 MHz): δ/ppm = 6.98 (s, 2H); ^{19}F NMR ($CDCl_3$, 400 MHz): δ/ppm = − 142.9 (m, 2F, *ortho*), − 1502.9 (t, 1F, *para*), − 160.9 (m, 2F, *meta*). There was evidence of ~ 1 % impurity (the ring-opened intermediate) by the presence of a small doublet at ~ 6.75 ppm in the ^{1}H NMR spectrum.

RAFT Copolymerization of PFS and NMI. A series of copolymers with different starting feed concentrations of PFS and NMI were prepared as per Table 1. In all cases the targeted [monomer]:[CPADB]:[ACVA] ratio was held constant at 300:1:0.2; differing ratios of PFS and NMI were used to target a particular copolymer composition. In a 25 mL round-bottomed flask, NMI, ACVA and CPADB were combined, followed by the addition of 1,4-dioxane (10 mL) to dissolve all solids. PFS was added to the flask via micropipette, which was sealed with rubber septa and degassed via bubbling with either nitrogen or argon for approximately 30 minutes on

ice. The targeted solids content (assuming 100 % conversion of monomer to polymer) was 10 % w/w. Polymerization was conducted for 18 hours at 70°C with constant magnetic stirring (400 rpm). Opening the reaction flask followed by immersion in an ice bath quenched the polymerization. Fractional conversion of monomer to polymer was determined via ^{1}H NMR in $CDCl_3$ (see Polymer Characterization). The resultant copolymers were purified by precipitation twice into excess methanol from 1,4-dioxane and dried in a vacuum oven at 30°C.

RAFT Copolymerization of PFPMI with PFS and Styrene. For both the copolymerization of PFPMI with styrene and of PFPMI with PFS, a 30:70 mole ratio of PFPMI to other monomer was targeted. The polymerization procedure was analogous to that described above, where CPADB was used as the RAFT agent and the targeted [monomer]:[CPADB]:[ACVA] ratio was 300:1:0.2, however the PS-PFPMI and PFS-PFPMI copolymerizations were allowed to proceed for 24 and 48 hours at 70 °C respectively. The resultant copolymers were purified by precipitation twice into excess methanol and isolated by vacuum filtration and dried in a vacuum oven at 30°C.

Polymer Characterization. 600 MHz Bruker Avance III, 400 MHz Bruker Avance III and 300 MHz Bruker Avance III NMR spectrometers were used to characterize PFPMI and copolymers prepared in this study. Fractional conversion of PFS and NMI (or PFPMI) was calculated by considering the integral of the vinylic and maleimide protons of the two monomers (δ = 5.7, 6.0 ppm and δ = 6.85, 6.98 ppm respectively) before and after polymerization, relative to 1,3,5-trioxane as an internal reference (δ = 5.15 ppm).[38] Due to the fluorinated nature of the copolymers synthesised, ^{1}H, ^{13}C and ^{19}F nuclei were studied. Details of 2D NMR spectral acquisition are provided in the Supporting Information.

A Shimadzu SEC system consisting of four Phenogel columns (10^5, 10^4, 10^3 and 500 Å pore size) was used to measure the molecular weight distribution of all synthesized copolymers, with tetrahydrofuran (THF) used as the eluent (flow rate 1 mL min^{-1}). Prior to analysis, all polymer samples were dissolved in THF to a concentration of 3 mg mL^{-1} and subsequently filtered through a 0.45 μm nylon filter. The columns were kept at 40°C by the CTO-10AC VP Shimadzu Column Oven. Polystyrene standards (Polymer Laboratories), with molar masses ranging from 0.58 to 1820 kDa, were used to calibrate the system.

X-ray photoelectron spectroscopy (XPS) was performed on an ESCALAB250Xi X-ray photoelectron spectrometer (Thermo Scientific, UK). The incident radiation was A1 X-rays (1486.6 eV) at 150 W (13 kV, 12 mA). A 165 mm hemispherical electron energy analyzer was used, with survey scans being taken at an analyzer pass energy of 100 eV over a 1360–0 eV binding energy range with 1.0 eV steps and a dwell time of 100 ms. Higher resolution scans were taken at a at 20 eV analyzer pass energy with 0.1 eV steps and a dwell time of 250 ms. Base pressure in the analysis chamber was below 1.5 x 10^{-9} Torr and during sample analysis 1.0 x 10^{-8} Torr. The data was analyzed using the Avantage software suite (Thermo Scientific).

Fourier transform infrared (FTIR) spectra were acquired using a PerkinElmer FTIR spectrometer, fitted with a microscope and attenuated total reflectance accessories. The absorbance and transmittance of each sample was measured over a wavenumber range of 400 – 5000 cm^{-1}; 64 scans per sample were recorded.

Polymer glass transition temperature (T_g) values were determined using a PerkinElmer STA 6000 differential scanning calorimeter (DSC). Three heating and cooling curves between 25°C and 300°C at a heating rate of 20°C min^{-1} were collected for each polymer sample.

449 The thermal decomposition profile of each of the polymers was determined by
450 thermogravimetric analysis (TGA) using a TGA Q5000 instrument (PolyScience, V3.15 Build
451 263). Each sample was heated to 800°C at a rate of 10°C min^{-1} under a nitrogen atmosphere (25
452 mL min^{-1}).

453 **Preparation of Polymer Films via Spin Coating.** Cut Si wafers were subjected to a rigorous
454 cleaning protocol prior to spin coating.[39] First, individual wafers were subjected to sequential
455 sonication for 1 minute in distilled ethanol and then in distilled acetone and dried with high
456 purity N_2 gas between each immersion. Each wafer was then treated with a carbon dioxide snow
457 jet to remove further contaminants, and finally 1 minute of plasma treatment (Harrick Plasma
458 PDC-001) to fully remove adsorbed contaminants on the Si substrate. The cleaned Si wafers
459 were coated with polymers by spin-coating with a Laurell Technologies WS-400B-6NPP/LITE
460 spin coater. Solutions of PFS-NMI copolymers in acetone and PFPMI copolymers in THF were
461 prepared to concentrations of 10 mg mL^{-1} and filtered through a 0.45 μm nylon filter. Polymer
462 monolayers were prepared by spin-coating these solutions (30 μL dispensed volume) on to the Si
463 wafers at 3000 rpm for 60 sec. All cleaning procedures and spin-coating were performed inside a
464 laminar flow cabinet.

465 **Thin Film Characterization.** The thickness and refractive indexes of the polymer films were
466 determined using a J.A. Woollam Co. spectroscopic ellipsometer (Model 2000V). The angle of
467 incidence was 75° and at least three measurements performed per polymer sample.

468 The wettability of the fabricated polymer monolayers was determined by measuring the static
469 and dynamic contact angles with water using a KSV CAM200 contact angle goniometer. Static
470 contact angles were determined by dispensing a 3 μL droplet of water (Milli-Q grade) onto the

polymer film. Advancing contact angles were determined by the addition of 5 μL of water to the droplet at a rate of 0.2 μL s^{-1}. The receding contact angle behaviour was determined using an analogous procedure. Measurements were performed on three different spots on each substrate.

Thermal annealing of polymer films was performed using a TR-124 hot plate (ATV Technologies, Munich) in air.

The spin-coated surfaces were analysed in air by a Bruker Dimension Atomic Force Microscope in ScanAsyst™ mode, using triangular SCANASYST-AIR AFM tips. The instrument was operated in tapping mode with a scan rate of 1 Hz and a nominal force constant of 0.4 N m^{-1}. The root mean square roughness (R_{RMS}) and topography of the surfaces was determined over an area that was typically 30 μm × 30 μm.

ASSOCIATED CONTENT

Supporting Information. XPS Spectra, accompanying NMR spectra, TGA profiles of PFPMI-based polymers, ellipsometric data, AFM topographical images.

ACKNOWLEDGMENT

Funding from the Australian Research Council Linkage Grants scheme (LP130100088) is gratefully acknowledged. Funding of the NMR Facility at the Central Science Laboratory at the University of Tasmania through the Australian Research Council Linkage Infrastructure, Equipment and Facilities Grants Scheme (LE120100018) is also gratefully acknowledged. S.T.

acknowledges the University of New South Wales for the provision of a Vice-Chancellor's Post-Doctoral Research Fellowship.

REFERENCES

[1] L. Feng, S. Li, Y. Li, H. Li, L. Zhang, J. Zhai, Y. Song, B. Liu, L. Jiang, D. Zhu, *Advanced Materials*, **2002**, *14*, 1857.
[2] A. Nakajima, A. Fujishima, K. Hashimoto, T. Watanabe, *Advanced Materials*, **1999**, *11*, 1365.
[3] M. Nosonovsky, B. Bhushan, *Current Opinion in Colloid & Interface Science*, **2009**, *14*, 270.
[4] M. Sadat-Shojai, A. Ershad-Langroudi, *Journal of Applied Polymer Science*, **2009**, *112*, 2535.
[5] (a) S. C. Thickett, C. Neto, A. T. Harris, *Advanced Materials*, **2011**, *23*, 3718; (b) M. Ghezzi, S. C. Thickett, A. M. Telford, C. D. Easton, L. Meagher, C. Neto, *Langmuir*, **2014**, *30*, 11714; (c) S. C. Thickett, J. Moses, J. R. Gamble, C. Neto, *Soft Matter*, **2012**, *8*, 9996.
[6] S. Agarwal, M. Becker, F. Tewes, *Polymer International*, **2005**, *54*, 1620.
[7] (a) L. Feng, S. Li, H. Li, J. Zhai, Y. Song, L. Jiang, D. Zhu, *Angewandte Chemie International Edition*, **2002**, *114*, 1269; (b) J.-Y. Shiu, C.-W. Kuo, P. Chen. in *Proceedings of SPIE-The International Society for Optical Engineering* **2005,** pp. 325-332.
[8] (a) I. S. Bayer, A. J. Davis, A. Biswas, *RSC Advances*, **2014**, *4*, 264; (b) H. Y. Erbil, A. L. Demirel, Y. Avcı, O. Mert, *Science*, **2003**, *299*, 1377; (c) J. Jiang, L. Zhu, L. Zhu, B. Zhu, Y. Xu, *Langmuir*, **2011**, *27*, 14180.
[9] R. P. Garrod, L. G. Harris, W. C. E. Schofield, J. McGettrick, L. J. Ward, D. O. H. Teare, J. P. S. Badyal, *Langmuir*, **2007**, *23*, 689.
[10] C. Dorrer, J. Rühe, *Langmuir*, **2008**, *24*, 6154.
[11] L. M. Han, R. B. Timmons, W. W. Lee, Y. Chen, Z. Hu, *Journal of Applied Physics*, **1998**, *84*, 439.
[12] (a) C. C. Ibeh. *Thermoplastic Materials: Properties, Manufacturing Methods, and Applications* **2014** (CRC Press: Florida); (b) D. K. Owens, R. Wendt, *Journal of Applied Polymer Science*, **1969**, *13*, 1741.
[13] (a) S. K. Papadopoulou, C. Michailof, I. Karapanagiotis, I. Zuburtikudis, C. Panayiotou. in *American Institute of Chemical Engineers 2008 Annual Meeting* **2008**; (b) E. Alyamac, M. D. Soucek, *Progress in Organic Coatings*, **2011**, *71*, 213.
[14] G. Odian. *Principles of Polymerization* **2004** (Wiley Interscience).
[15] J. A. Brydson. *Plastics Materials* **2013** (Elsevier Science).
[16] (a) J. M. Barrales-Rienda, J. I. G. De La Campa, J. G. Ramos, *Journal of Macromolecular Science: Part A - Chemistry*, **1977**, *11*, 267; (b) M. Yoshihara, J.-I. Asakura, H. Takahashi, T. Maeshima, *Journal of Macromolecular Science: Part A - Chemistry*, **1983**, *20*, 123; (c) A. A. Mohamed, F. H. Jebrael, M. Z. Elsabee, *Macromolecules*, **1986**, *19*, 32; (d) C. P. R. Nair, D. Mathew, K. N. Ninan, *European Polymer Journal*, **1999**, *35*, 1829; (e) F. Yilmaz, L. Cianga, Y. Guner, L. Topppare, Y. Yagci, *Polymer*, **2004**, *45*, 5765; (f) L. Lou, Y. Koike, Y.

Okamoto, *Polymer*, **2011**, *52*, 3560; (g) A. Matsumoto, T. Kubota, T. Otsu, *Macromolecules*, **1990**, *23*, 4508.
[17] (a) B. D. Dean, *Journal of Applied Polymer Science*, **1987**, *33*, 2259; (b) Y. Yuan, A. Siegmann, M. Narkis, J. Bell, *Journal of Applied Polymer Science*, **1996**, *61*, 1049; (c) A. Matsumoto, T. Kubota, T. Otsu, *Macromolecules*, **1990**, *23*, 4508.
[18] J. Barrales-Rienda, J. G. Ramos, M. S. Chaves, *Journal of Polymer Science: Polymer Chemistry Edition*, **1979**, *17*, 81.
[19] Y. Fu, Y.-T. R. Lau, L.-T. Weng, K.-M. Ng, C.-M. Chan, *Journal of Colloid and Interface Science*, **2014**, *431*, 180.
[20] (a) W. A. Pryor, T.-L. Huang, *Macromolecules*, **1969**, *2*, 70; (b) N. ten Brummelhuis, M. Weck, *ACS Macro Letters*, **2012**, *1*, 1216; (c) N. t. Brummelhuis, M. Weck, *Journal of Polymer Science Part A: Polymer Chemistry*, **2014**, *52*, 1555.
[21] C. Pugh, C. N. Tang, M. Paz-Pazos, O. Samtani, A. H. Dao, *Macromolecules*, **2007**, *40*, 8178.
[22] (a) J. Chiefari, Y. Chong, F. Ercole, J. Krstina, J. Jeffery, T. P. Le, R. T. Mayadunne, G. F. Meijs, C. L. Moad, G. Moad, *Macromolecules*, **1998**, *31*, 5559; (b) G. Moad, E. Rizzardo, S. H. Thang, *Australian Journal of Chemistry*, **2006**, *59*, 669; (c) G. Moad, E. Rizzardo, S. H. Thang, *Polymer*, **2008**, *49*, 1079.
[23] K. Matyjaszewski, N. V. Tsarevsky, *Journal of the American Chemical Society*, **2014**, *136*, 6513.
[24] J. Nicolas, Y. Guillaneuf, C. Lefay, D. Bertin, D. Gigmes, B. Charleux, *Progress in Polymer Science*, **2013**, *38*, 63.
[25] G.-Q. Chen, Z.-Q. Wu, J.-R. Wu, Z.-C. Li, F.-M. Li, *Macromolecules*, **2000**, *33*, 232.
[26] A. Li, J. Lu, *Journal of Applied Polymer Science*, **2009**, *114*, 2469.
[27] P. Yang, L. P. D. Ratcliffe, S. P. Armes, *Macromolecules*, **2013**, *46*, 8545.
[28] M. Alger. *Polymer Science Dictionary* **1996** (Springer: The Netherlands).
[29] (a) H. Adams, J.-L. Jimenez Blanco, G. Chessari, C. A. Hunter, C. M. R. Low, J. M. Sanderson, J. G. Vinter, *Chemistry – A European Journal*, **2001**, *7*, 3494; (b) H. Adams, J. L. Jimenez Blanco, G. Chessari, C. A. Hunter, C. M. Low, J. M. Sanderson, J. G. Vinter, *Chemistry- A European Journal*, **2001**, *7*, 10.
[30] M. P. Callahan, Z. Gengeliczki, N. Svadlenak, H. Valdes, P. Hobza, M. S. de Vries, *Physical Chemistry Chemical Physics*, **2008**, *10*, 2819.
[31] P. C. Hiemenz, T. P. Lodge. *Polymer Chemistry* **2007** (CRC press: Florida).
[32] G. Liu, X. Li, L. Zhang, X. Qu, P. Liu, L. Yang, J. Gao, *Journal of Applied Polymer Science*, **2002**, *83*, 417.
[33] J. Rieger, *Journal of Thermal Analysis*, **1996**, *46*, 965.
[34] P. Sivasamy, M. Meenakshisundaram, and C. T. Vijayakumar, *Journal of analytical and applied pyrolysis*, **2003**, 9.
[35] S. C. Siah, B. Hoex, A. G. Aberle, *Thin Solid Films*, **2013**, *545*, 451.
[36] (a) P. Müller-Buschbaum, J. S. Gutmann, M. Wolkenhauer, J. Kraus, M. Stamm, D. Smilgies, W. Petry, *Macromolecules*, **2001**, *34*, 1369; (b) K. E. Strawhecker, S. K. Kumar, J. F. Douglas, A. Karim, *Macromolecules*, **2001**, *34*, 4669.
[37] T. Garel, L. Leibler, H. Orland, *Journal de Physique II*, **1994**, *4*, 2139.
[38] J. W. Emsley, Feeney, J., Sutcliffe, L.H. in *High Resolution NMR Spectroscopy* **1966**, (Pergamon Press: Oxford).

[39] C. Neto, K. Jacobs, R. Seemann, R. Blossey, J. Becker, G. Gruen, *Journal of Physics: Condensed Matter*, **2003**, *15*, 3355.